BBA - Molecular Basis of Disease 1865 (2019) 2526–2537

Contents lists available at ScienceDirect

BBA - Molecular Basis of Disease

journal homepage: www.elsevier.com/locate/bbadis

Impact of hyperinsulinemia and hyperglycemia on valvular interstitial cells – A link between aortic heart valve degeneration and type 2 diabetes

Jessica I. Selig[a], D. Margriet Ouwens[b,c,d], Silja Raschke[a], G. Hege Thoresen[e,f], Jens W. Fischer[g], Artur Lichtenberg[a], Payam Akhyari[a,*], Mareike Barth[a]

[a] Department of Cardiovascular Surgery, Medical Faculty, University Hospital Düsseldorf, Heinrich-Heine-University, Düsseldorf, Germany
[b] Institute of Clinical Biochemistry and Pathobiochemistry, German Diabetes Center, Düsseldorf, Germany
[c] German Center for Diabetes Research, München-Neuherberg, Germany
[d] Department of Endocrinology, Ghent University Hospital, Ghent, Belgium
[e] Department of Pharmaceutical Biosciences, School of Pharmacy, University of Oslo, Oslo, Norway
[f] Department of Pharmacology, Institute of Clinical Medicine, University of Oslo, Oslo, Norway
[g] Department of Pharmacology and Clinical Pharmacology, Medical Faculty, University Hospital Düsseldorf, Heinrich-Heine-University, Düsseldorf, Germany

ARTICLE INFO

Keywords:
Valvular interstitial cells
Insulin sensitivity
Hyperglycemia
Diabetes

ABSTRACT

Type 2 diabetes is a known risk factor for cardiovascular diseases and is associated with an increased risk to develop aortic heart valve degeneration. Nevertheless, molecular mechanisms leading to the pathogenesis of valve degeneration in the context of diabetes are still not clear. Hence, we hypothesized that classical key factors of type 2 diabetes, hyperinsulinemia and hyperglycemia, may affect signaling, metabolism and degenerative processes of valvular interstitial cells (VIC), the main cell type of heart valves. Therefore, VIC were derived from sheep and were treated with hyperinsulinemia, hyperglycemia and the combination of both. The presence of insulin receptors was shown and insulin led to increased proliferation of the cells, whereas hyperglycemia alone showed no effect. Disturbed insulin response was shown by impaired insulin signaling, i.e. by decreased phosphorylation of Akt/GSK-3α/β pathway. Analysis of glucose transporter expression revealed absence of glucose transporter 4 with glucose transporter 1 being the predominantly expressed transporter. Glucose uptake was not impaired by disturbed insulin response, but was increased by hyperinsulinemia and was decreased by hyperglycemia. Analyses of glycolysis and mitochondrial respiration revealed that VIC react with increased activity to hyperinsulinemia or hyperglycemia, but not to the combination of both. VIC do not show morphological changes and do not acquire an osteogenic phenotype by hyperinsulinemia or hyperglycemia. However, the treatment leads to increased collagen type 1 and decreased α-smooth muscle actin expression. This work implicates a possible role of diabetes in early phases of the degeneration of aortic heart valves.

1. Introduction

Type 2 diabetes is a growing epidemic with an estimated doubling of its prevalence until 2030 [1]. Cardiovascular complications represent a major cause for morbidity and mortality in patients with type 2 diabetes [2,3]. Impaired insulin sensitivity in combination with hyperglycemia represents an important trigger that underlies degenerative processes in the cardiovascular system of patients with type 2 diabetes [4–6]. For example, diabetic cardiomyopathy is a well-known complication of type 2 diabetes, and is characterized by functional and structural alterations in the myocardium often accompanied by metabolic dysfunction [7–13]. Besides myocardial injury, animal models also suggest a link between diabetes and degeneration of the aortic valve [14]. Retrospective and prospective clinical studies provide some evidence for an association of diabetes with an increased risk of developing severe aortic valve stenosis [15,16] and indicate that diabetes may represent a predicting factor for the development of aortic valve stenosis [17]. Here, diabetes has been shown to be significantly and independently associated with the risk of developing severe aortic valve stenosis. This clinical association is alarming on the socioeconomic

* Corresponding author at: Department of Cardiovascular Surgery, Medical Faculty, University Hospital Düsseldorf, Heinrich-Heine-University, Moorenstraße 5, 40225 Düsseldorf, Germany.
E-mail addresses: Jessica.Selig@med.uni-duesseldorf.de (J.I. Selig), Margriet.Ouwens@ddz.de (D.M. Ouwens), Hege.Thoresen@farmasi.uio.no (G.H. Thoresen), Jens.Fischer@uni-duesseldorf.de (J.W. Fischer), Artur.Lichtenberg@med.uni-duesseldorf.de (A. Lichtenberg), Payam.Akhyari@med.uni-duesseldorf.de (P. Akhyari), Mareike.Barth@med.uni-duesseldorf.de (M. Barth).

https://doi.org/10.1016/j.bbadis.2019.05.019
Received 12 January 2019; Received in revised form 27 April 2019; Accepted 28 May 2019
Available online 30 May 2019

level considering the increasing prevalence of diabetes. Moreover, published meta-analyses have shown that 'pre-diabetes', a status associated with disturbances in insulin action before clinically relevant diabetes becomes evident, is associated with an increased risk for cardiovascular diseases [18]. Despite the close associations between diabetes and cardiovascular damage, little is known concerning the molecular impact of diabetes on hemostasis and remodeling of the aortic valve. Thus, insulin action and the impact of hyperglycemia on the aortic valve are of vital interest for a better understanding of the underlying mechanisms and the pathology in the onset of degeneration of the aortic valve.

The aortic heart valve is composed of extracellular matrix components and is covered with endothelial cells [19,20]. Valvular interstitial cells (VIC) are loosely interspersed in the valve interior and represent the main cell type of the aortic valve. VIC display phenotypic changes under the pathologic conditions of aortic valve stenosis and calcification. Accordingly, VIC are considered as a representative model for the study of the pathophysiological mechanisms contributing to aortic valve disorders [21]. The aim of this study was to detail the impact of diabetes on these cells with emphasis on the question whether and how VIC react to hyperglycemia and hyperinsulinemia. Therefore, we exposed primary ovine VIC to chronic hyperglycemia with or without hyperinsulinemia and examined the impact of these pathophysiological stimuli on determinants of metabolic (dys)function, such as insulin sensitivity, cell proliferation, glucose metabolism, mitochondrial function and degenerative processes.

2. Materials and methods

2.1. Isolation and culture of primary ovine VIC

Hearts of 6–8 months old male sheep ($n = 6$) were obtained from a local abattoir and the individual leaflets of the aortic valve were freshly excised. After rinsing in PBS, the leaflets were minced in small pieces and incubated in Dulbecco's modified Eagle's medium with GlutaMAX supplement (DMEM; Invitrogen, Carlsbad, CA, USA) including 10% fetal calf serum (FCS; Sigma-Aldrich, St. Louis, MO, USA), 1% penicillin/streptomycin (Invitrogen) and 1% non-essential amino acids either (Sigma-Aldrich) in normoglycemic control medium (DMEM containing 1 g/L glucose) or in hyperglycemic medium (DMEM containing 4.5 g/L glucose) at 37 °C and 5% CO_2. Outgrown VIC were passaged three to four times to increase cell number. At confluency, VIC were seeded in gelatin-coated 6-well plates and treated with 100 nM insulin (cat. no.: I5523; Sigma-Aldrich) with medium changes every second day. Cells were counted using a Neubauer chamber and trypan blue (Sigma-Aldrich). Cell count was determined every second day. For immunohistochemical stainings of cultured cells, VIC were seeded on gelatin-coated glass cover slips (10 mm in diameter; Glaswarenfabrik Karl Hecht KG, Sondheim, Germany) placed in 6-well plates and cultured for five days using the aforementioned treatments. Transmitted light images of cultured cells were taken prior to fixation by an Invers DM IL Type LED microscope and a DFC425C camera using LAS version 3.8 software (Leica, Wetzlar, Germany). Cells on cover slips were washed with warm PBS, fixed with ice-cold methanol for 5 min following ice-cold acetone for 20 s (both Carl Roth, Karlsruhe, Germany) and stored at −20 °C until staining.

2.2. Acute insulin stimulus

Supernatant was aspirated and cells were washed twice with PBS. Then, cells were starved for 4 h in DMEM w/o FCS. After starvation, cells were treated with 100 nM insulin for 10 min, followed by two washing steps with ice-cold PBS. Cells were lysed in 50 mM HEPES (pH 7.4) containing 1% TX100 and PhosSTOP/cOmplete Protease Inhibitor Cocktail (Roche, Basel, Switzerland).

2.3. SDS-PAGE and Western blot analysis

All experiments were conducted after five days of treatment. Lysates were mixed with Roti-Load (Roth, Karlsruhe, Germany). Proteins were separated on a 10% reducing SDS-polyacrylamide gel and blotted on nitrocellulose. Detection of protein signals was performed with primary antibodies against Akt (cat. no.: C67E7/4691; Cell Signaling, Danvers, MA, USA), phospho-Akt(Ser^{473}) (cat. no.: 4060; Cell Signaling), GSK-3α/β (cat. no.: 5676; Cell Signaling) and phospho-GSK-3α/β (Ser^{21}/Ser^{9}) (cat. no.: C7154; LifeSpanBiosciences, Seattle, WA, USA), GLUT1 (cat. no.: ab14683; Abcam, Cambridge, UK) and GLUT4 (cat. no.: ab654; Abcam). For normalization, detection of housekeeper protein signals was performed on the according nitrocellulose membranes with primary antibodies against β-tubulin (cat. no.: T7816; Sigma-Aldrich) or β-actin (cat. no.: A5316; Sigma-Aldrich). For detection of primary antibody signals the following secondary antibodies were used: IRDye 800 CW goat anti rabbit (cat. no.: 926-32211), IRDye 680 LT goat anti mouse (cat. no.: 926-68020, LI-COR biosciences, Lincoln, NE, USA). PageRuler Prestained Protein ladder (cat. no.: 26616; Thermo Fisher Scientific, Waltham, MA, USA) was used for determination of molecular weight. Analysis was performed by using an Odyssey scanner (LI-COR biosciences) and intensity of protein bands was expressed as arbitrary units (AU). Depicted representative Western blots were cropped for clarity reasons since there have been other treatments tested, which showed no regulation and which are shown in total in the supplemental materials part.

2.4. Glucose measurements

Measurements of glucose concentrations in the cell culture supernatants were performed in duplicates every day using a GLUCO Smart Swing blood glucose meter and test strips (MSP Bodmann, Bobingen, Germany).

2.5. Glucose uptake assay

Glucose uptake measurements were performed using the Glucose Uptake-Glo Assay (cat. no.: J1341, Promega, Madison, WI, USA) according to the manufacturer's instructions. Therefore, VIC were cultured until day 5 under normo- or hyperglycemic conditions with or w/o chronic insulin stimulus as described above. After starvation for 18 h in DMEM w/o FCS, VIC were washed twice with PBS followed by an acute insulin stimulus with 100 nM insulin for 1 h. Afterwards, the supernatant was discarded and the cells were incubated with 500 μM 2-deoxyglucose for 12 min. Reaction was stopped and the cells were lysed. Detection Reagent was added and incubated for 30 min. Then, bioluminescence was measured for 750 ms after 4 h at a microplate reader (Infinite M1000 Pro, Tecan, Männedorf, Switzerland). Obtained values were corrected for background signal (PBS w/o 2-deoxyglucose) and normalized to the appropriate condition.

2.6. mRNA isolation and semi-quantitative real-time PCR analysis

Myocardium, liver and aortic valve leaflets were obtained from a local abattoir. The tissues were freshly cyro-preserved by snap-freezing in 2-methylbutane (Sigma-Aldrich) cooled to the temperature of liquid nitrogen and storage at −80 °C upon usage. Total RNA of tissues was isolated by TRIzol reagent according to the manufacturer's instructions and subsequent RNA purification using the QIAGEN RNeasy mini kit (QIAGEN, Venlo, Netherlands). Total RNA of VIC was isolated by using directly the QIAGEN RNeasy mini kit. cDNA synthesis was performed with QIAGEN Quantitect reverse transcription kit. Semi-quantitative real-time PCR was performed with a StepOnePlus Real-Time PCR System (Applied Biosystems, Waltham, MA, USA) by using the Platinum SYBR Green qPCR SuperMix-UDG/ROX kit (Invitrogen). PCR protocol was as follows: starting with an initial step for 2 min at 50 °C, followed

Table 1
Primer sequences.

Gene	Forward sequences (5′-3′)	Reverse sequences (5′-3′)
RPL29	CCAAGTCCAAGAACCACACC	TATCGTTGTGATCGGGGTTT
INSR	GGCGGAAGATAGTGAGCTGTA	CACTCTGGTTGTGCTTCTGG
IGF1R	GACGGAGCCTGTGTTCTTCT	CAGAGCAATCATCAGGTGGA
GLUT1	GCACCAGCTAGGCATCGT	GGGATGAAGATGACGCTCAG
GLUT2	TGGACGGGCAATTTCATTAT	GTAAAGGCCAAGACCACACC
GLUT4	CCCCGCTACCTCTACATCAT	CTCAGCCAACACCTCAGACA
ACTA2	TAGAACACGGCATCATCACC	TGAGAAGGGTTGGATGCTCT
COL1A1	AAGACATCCCACCAGTCACC	TAAGTTCGTCGCAGATCACG
SPP1	AATACCCAGATGCTGTAGCCA	TAGATCGTCTGTTTGCTCAGG

by 2 min at 95 °C. 40 cycles were performed with 15 s at 95 °C and 30 s at 60 °C followed by single steps for 15 s at 95 °C, 1 min at 60 °C and 15 s at 95 °C (primer sequences are shown in Table 1). The comparative $2^{-\Delta\Delta Ct}$ method was used for analysis of relative gene expression.

2.7. Glycolytic rate analysis and mitochondrial stress assay

Determinants of glycolysis and mitochondrial function were examined in living cells using a Seahorse XFe96 extracellular flux analyzer (Agilent Technologies, Santa Clara, CA, USA), which measures extracellular acidification rates (ECAR) and oxygen consumption rates (OCR) during the oxidation of energy substrates. For each assay, cells were plated at a density of 750 cells per well in XFe96-well microplates (Agilent Technologies), and cultured for five days under normo- or hyperglycemic conditions with or without hyperinsulinemia as described above (see Section 2.1). Before each assay, the cultures were washed twice with glycolytic rate assay medium consisting of Dulbecco's modified eagle's base medium (cat. no.: D5030, Sigma-Aldrich), supplemented with 5 mM glucose, 2 mM glutamine, 1 mM sodium pyruvate, and 5 mM HEPES (pH 7.4 at 37 °C). Then, 180 µL glycolytic rate assay medium was added to each well, and cells were placed for 4 h at 37 °C in a CO_2-free incubator. Mitochondrial function was examined from OCRs under basal conditions and in response to consecutive injections with 1 µM oligomycin A, 0.7 µM carbonyl cyanide-4-(trifluoromethoxy)phenylhydrazone (FCCP), and 0.5 µM rotenone/antimycin A (Seahorse XF Cell Mito Stress Test Kit, Agilent Technologies). The cell density as well as the optimal FCCP concentration was determined in a pilot experiment and judged on the basis of the increase in OCR after injection with FCCP. For the analysis of glycolysis, ECAR and OCR were recorded under basal conditions and in response to consecutive injections with 100 nM insulin, 0.5 µM rotenone/antimycin A and 50 mM 2-deoxyglucose (Seahorse XF Glycolytic Rate Assay Kit, Agilent Technologies). All data were analyzed with WAVE software (version 2.6.0.31, Agilent Technologies) to calculate the determinants of glycolysis and mitochondrial function in the various assays using the following formulas:

2.7.1. Glycolysis

Prior to analysis, the ECAR recordings were converted in proton exchange rates (PER), a metric for extracellular acidification that accounts for buffer capacity of the medium and plate geometry [22]. The obtained PER values were used to calculate determinants of glycolysis as follows:

Mitochondrial PER = CO_2 conversion factor * (OCR − minimum OCR after rotenone/antimycin A injection), in which the CO_2 conversion factor for XFe96 well plates is defined as 0.61 [22].
Glycolytic PER = total PER − mitochondrial PER
Basal glycolysis = last glycoPER before injection with insulin
Basal PER = last PER before injection with insulin
% PER from glycolysis = (basal glycolysis/basal PER) ∗ 100%
Compensatory glycolysis = maximum glycoPER after rotenone/antimycin A injection
MitoOCR/glycoPER = (last OCR before the first injection − minimum OCR after rotenone/antimycin A injection)/basal glycolysis
Post 2-deoxyglucose acidification = minimum glycoPER after injection with 2-deoxyglucose
Insulin-stimulated glycolysis = average glycoPER after insulin injection and before rotenone/antimycin A injection
Insulin-stimulated PER = average PER after insulin injection and before rotenone/antimycin A injection

2.7.2. Mitochondrial function

Non-mitochondrial respiration = minimum OCR after rotenone/antimycin A injection
Basal respiration = last OCR before injection of oligomycin − non-mitochondrial respiration
Maximal respiration = maximum OCR after FCCP injection − non-mitochondrial respiration
Spare respiratory capacity = maximal respiration − basal respiration
Proton leak = minimum OCR after oligomycin injection − non-mitochondrial respiration
ATP production = last OCR before injection of oligomycin − minimum OCR after injection of oligomycin
Coupling efficiency = (ATP production ∗ 100)/basal respiration

All data were normalized for protein content. Therefore, the medium was aspirated immediately after the assays, and cells were lysed by 3–4 freeze thaw cycles in 75 µL lysis buffer consisting of 10 mM Tris-HCl, 10 mM Na_2HPO_4, 10 mM NaH_2PO_4, 130 mM NaCl, 1% Triton X-100 (pH 7.5) followed by centrifugation for 5 min at 4000 rpm. Protein content was measured in 25 µL cell lysate using the Pierce BCA Protein Assay Kit (Thermo Fisher Scientific) according to the manufacturer's instructions.

2.8. Calcium assay

Calcium content of VIC was measured using a colorimetric calcium assay kit (cat. no.: KA1644, Abnova, Taipei, Taiwan) based on the complex formation of phenolsulphonephthalein with free calcium ions. Therefore, cells were washed in PBS and lysed in 100 mM Tris-HCl buffer (pH 7) containing 0.1% Triton-X-100. Lysates were incubated under rotation for 2 h at 4 °C and centrifuged at 13,000 rpm for 15 min at 4 °C. Extinctions of supernatants were measured at a microplate reader (Infinite M1000 Pro, Tecan) at 612 nm.

2.9. Immunohistochemistry

Fixed cells were incubated for 5 min in 0.1% Triton-X-100 in PBS, followed by three washing steps in PBS. Primary antibodies against vimentin (cat. no.: GP53, Progen, Heidelberg, Germany) and smooth muscle alpha actin (α-SMA; cat. no.: ab5694, Abcam) were incubated for 60 min, followed by three washing steps with PBS. Afterwards, cells were incubated with secondary fluorescent antibodies (Alexa488 and Alexa546; Dianova, Hamburg, Germany) for 30 min and 4′,6-diamidino-2-phenylindole (DAPI; cat. no.: 6335, Carl Roth) for 5 min and were washed three times with PBS. After rinsing the cover slips in aqua dest. for 1 min, cells were fixed with 100% ethanol and mounted on microscope slides. Immunofluorescent micrographs were taken using a DM2000 microscope, a DFC425C camera and LAS version 3.8 software (Leica).

2.10. Statistical analyses

For statistical analyses GraphPad Prism version 6.0 and 7.0

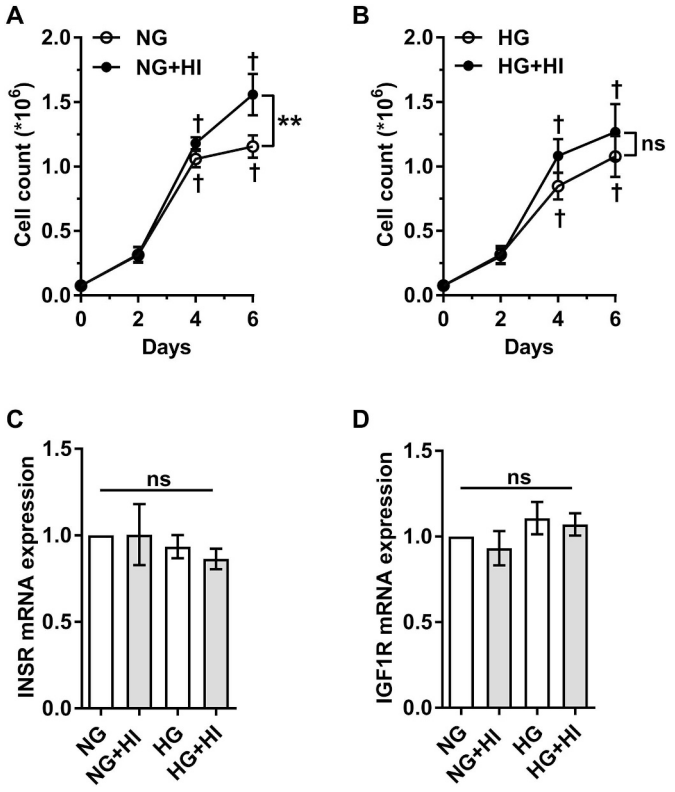

Fig. 1. Influence of insulin on proliferation rates and gene expression of insulin receptors.
Hyperinsulinemia led to significantly increased cell numbers at day six compared to untreated VIC under normoglycemic conditions (A), whereas the combination of hyperglycemia and hyperinsulinemia had no impact on cell proliferation (B). Gene expression analysis revealed expression of INSR (C) and IGF1R (D) in VIC. Neither hyperglycemia nor hyperinsulinemia had an influence on gene expression of INSR or IGF1R. Experiments were performed with VIC derived from $n = 6$ individual sheep. **: p-values < 0.01; †: p-values < 0.0001 compared to day 0; ns: not significant; NG: normoglycemia; HG: hyperglycemia; HI: hyperinsulinemia.

(GraphPad Software, San Diego, CA, USA) was used. Reported data are represented as mean with 95% confidence interval, except for proliferation and mRNA expression data in Figs. 1 and 7, where data are represented as mean ± standard error of mean. Statistical analysis was performed using 2way ANOVA with Sidak's multiple comparisons test.

3. Results

3.1. Impact of chronic insulin on proliferation of VIC

To investigate the proliferative influence of hyperinsulinemia, cell count was determined. Under normoglycemic conditions VIC were highly proliferative from day 2 to 6. On day 6 hyperinsulinemia led to a significantly higher cell count compared to untreated VIC (Fig. 1 A). Under hyperglycemic conditions VIC also show high proliferation rates, although there were no significant differences with addition of hyperinsulinemia (Fig. 1 B). Overall, the proliferative effect of insulin in the end-point was more pronounced under normoglycemic conditions (20% more cells) compared to hyperglycemia.

3.2. Expression of insulin receptors is not influenced by hyperinsulinemia or hyperglycemia

Gene expression analyses revealed the presence of insulin receptor and insulin-like growth factor 1 (IGF1) receptor. Treatment of cells with hyperinsulinemia and hyperglycemia showed no regulation of mRNA expression neither of the insulin receptor nor of the IGF1 receptor (Fig. 1C/D).

3.3. Effect of hyperinsulinemia and hyperglycemia on insulin action in VIC

Here we examined the effects of hyperinsulinemia and hyperglycemia on insulin sensitivity in VIC by examining the phosphorylation of Akt, a key component of signaling pathways controlling the metabolic actions of insulin [23]. In VIC cultured under normoglycemic conditions, acute insulin treatment (10 min, 100 nM) led to a 41-fold increase ($p < 0.001$) in the phosphorylation of Akt(Ser^{473}) (Fig. 2 A/B). Although chronic hyperinsulinemia did not affect basal phosphorylation of Akt(Ser^{473}), upon acute insulin stimulation the levels of phosphorylated Akt(Ser^{473}) were reduced by 52% ($p < 0.001$; Fig. 2 A/B). In VIC cultured under hyperglycemia, acute insulin treatment led to a 36-fold increase in the phosphorylation of Akt(Ser^{473}) ($p < 0.001$; Fig. 2 C/D). Additional chronic hyperinsulinemia reduced Akt(Ser^{473}) phosphorylation induced by acute insulin stimulation by 54% ($p < 0.001$; Fig. 2 C/D). Under normoglycemia, none of experimental conditions affected the protein abundance of total Akt (Fig. 2B right graph). Under hyperglycemic conditions, the addition of chronic hyperinsulinemia led to a minor decrease (6%) in total Akt abundance in the absence of acute insulin stimulation ($p < 0.05$; Fig. 2D right graph). Yet, the maximal levels achieved by chronic insulin treatment in cells cultured under hyperglycemia with acute insulin treatment were 27% lower as compared cells cultured under normoglycemic conditions ($p < 0.01$; Fig. 2 E). These data suggest a disturbed insulin response in VIC as indicated by lower levels of Akt phosphorylation.

To substantiate the data on insulin-mediated Akt(Ser^{473}) phosphorylation, we examined the effects of hyperinsulinemia and hyperglycemia on GSK phosphorylation (GSK-3α(Ser^{21}) and GSK-3β(Ser^{9})), a downstream target of Akt (Fig. 3). Under normoglycemic conditions, acute insulin stimulation promoted a 3.6- and 2.1-fold increase in the phosphorylation of GSK-3α(Ser^{21}) and GSK-3β(Ser^{9}), respectively (both $p < 0.001$). Chronic hyperinsulinemia had no effect on the basal phosphorylation state of GSK-3α/β(Ser^{21}/Ser^{9}) (Fig. 3 A-C). Although hyperinsulinemia impaired the phosphorylation of GSK-3α(Ser^{21}) induced by acute insulin stimulation by 20% ($p < 0.001$; Fig. 3 B), the insulin-mediated increase in phosphorylation of its isoform GSK-3β(Ser^{9}) was not impaired by hyperinsulinemia (Fig. 3 C). In VIC cultured under hyperglycemia, acute insulin treatment induced a 4.2- and 1.8-fold increase in the phosphorylation of GSK-3α(Ser^{21}) and GSK-3β(Ser^{9}), respectively (both $p < 0.001$). Combining hyperglycemia with chronic hyperinsulinemia not only further impaired the insulin-induced phosphorylation of GSK-3α(Ser^{21}) by 35% ($p < 0.001$; Fig. 3 E), but also impaired the insulin-induced phosphorylation of GSK-3β (Ser^{9}) by 18% ($p < 0.05$; fig. 3 F). None of the experimental conditions affected the protein abundances of total GSK-3α and GSK-3β.

3.4. Effect of hyperinsulinemia and hyperglycemia on glucose transport in VIC

The Akt pathway is a key regulator of insulin-regulated glucose metabolism [23]. To assess glucose uptake in VIC, we first examined the expression of glucose transporters in ovine aortic valve tissue. Using real-time PCR and Western blot analysis, it was found that aortic valve tissue expressed GLUT1, whereas GLUT2 and GLUT4 were not detectable. It should be noted that GLUT2 and GLUT4 were detected in ovine liver and myocardial samples, respectively (Fig. 4 A). Yet, the protein abundance of GLUT1 was not affected upon culturing the cells under conditions of hyperinsulinemia, hyperglycemia, or both versus normoglycemia (Fig. 4 B/C).

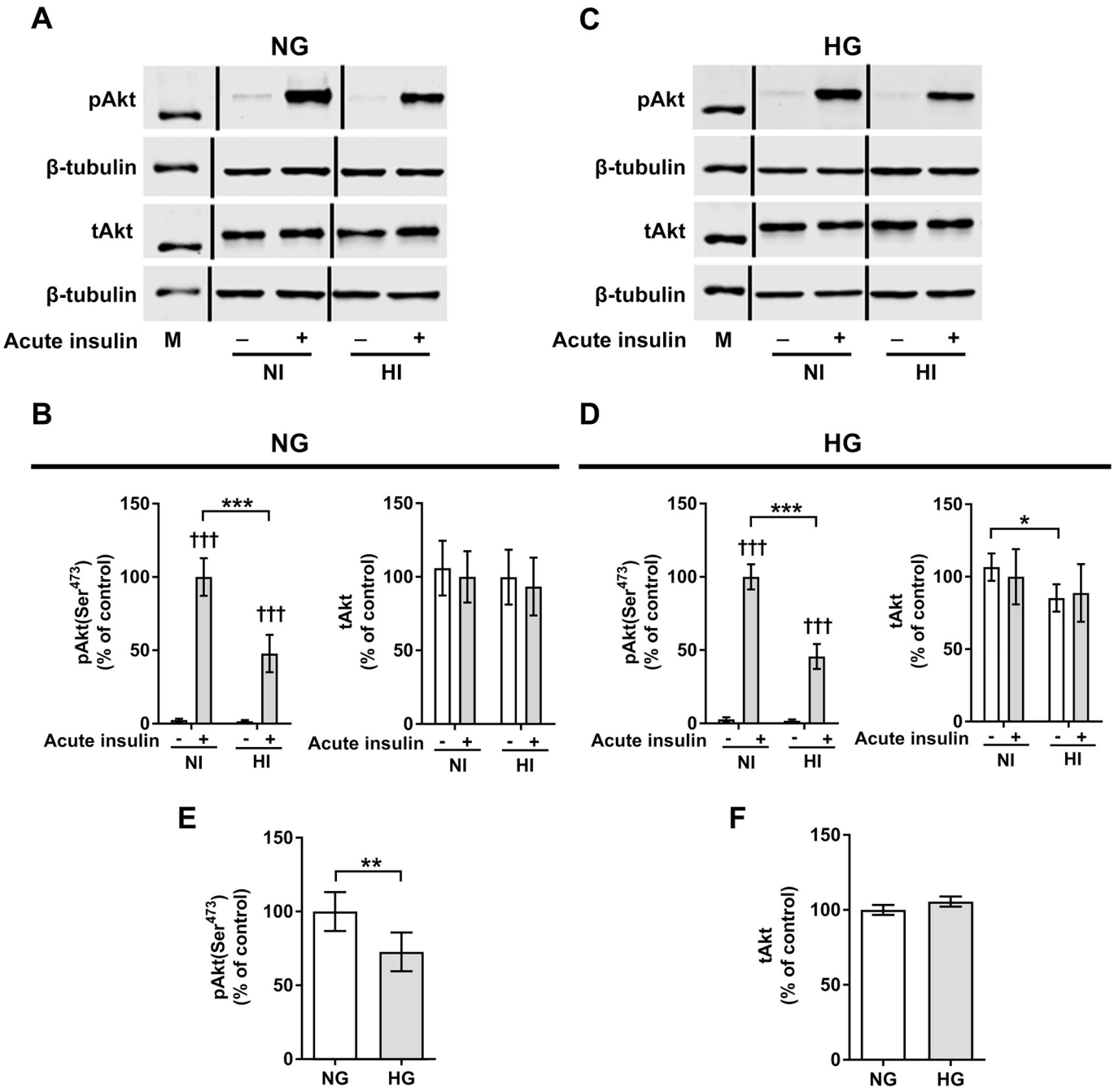

Fig. 2. Hyperinsulinemia impairs Akt phosphorylation in VIC.
Akt(Ser^{473}) phosphorylation upon chronic hyperinsulinemia is measured in VIC cultured under normoglycemic (A/B) or hyperglycemic conditions (C/D). Representative Western blot images show pAkt(Ser^{473}) and tAkt protein expression (A/C). Density analysis was performed for quantification of pAkt(Ser^{473}) and tAkt signals under normoglycemic (B) and under hyperglycemic conditions (D). Hyperinsulinemia led to significantly decreased phosphorylation of Akt(Ser^{473}) under normoglycemic (A/B) or hyperglycemic conditions (B/D). Maximal levels of pAkt(Ser^{473}) expression under normoinsulinemia with acute insulin stimulus were significantly lower under hyperglycemic conditions in comparison to normoglycemic conditions (E/F). Data were normalized to β-tubulin and expressed relative to control with acute insulin stimulus. Experiments were performed with VIC derived from $n = 6$ individual sheep. NG: normoglycemia; HG: hyperglycemia; NI: normoinsulinemia; HI: hyperinsulinemia; M: marker; *: p-values < 0.05 between indicated groups; †: p-values < 0.05 compared to the according basal condition without acute insulin stimulus. Lanes of protein ladder represent 55 kDa. Vertical black lines in A and C indicate non-adjacent bands which have been cropped since there has been an additional treatment in between non-essential to this work.

3.5. Glucose uptake assay

Glucose uptake assay (Fig. 4 D) showed that hyperinsulinemia leads to a nearly significantly higher glucose uptake under normoglycemic conditions (22%; $p = 0.053$), whereas the effect of hyperinsulinemia is abrogated under hyperglycemic conditions. Nevertheless, basal glucose uptake as well as glucose uptake under hyperinsulinemia was decreased under hyperglycemic conditions compared to normoglycemic treatment by 34% ($p < 0.05$) and by 35% ($p < 0.01$), respectively.

3.6. Effect of hyperinsulinemia and hyperglycemia on glycolysis and mitochondrial function

Using a Seahorse Analyzer, determinants of glycolysis and

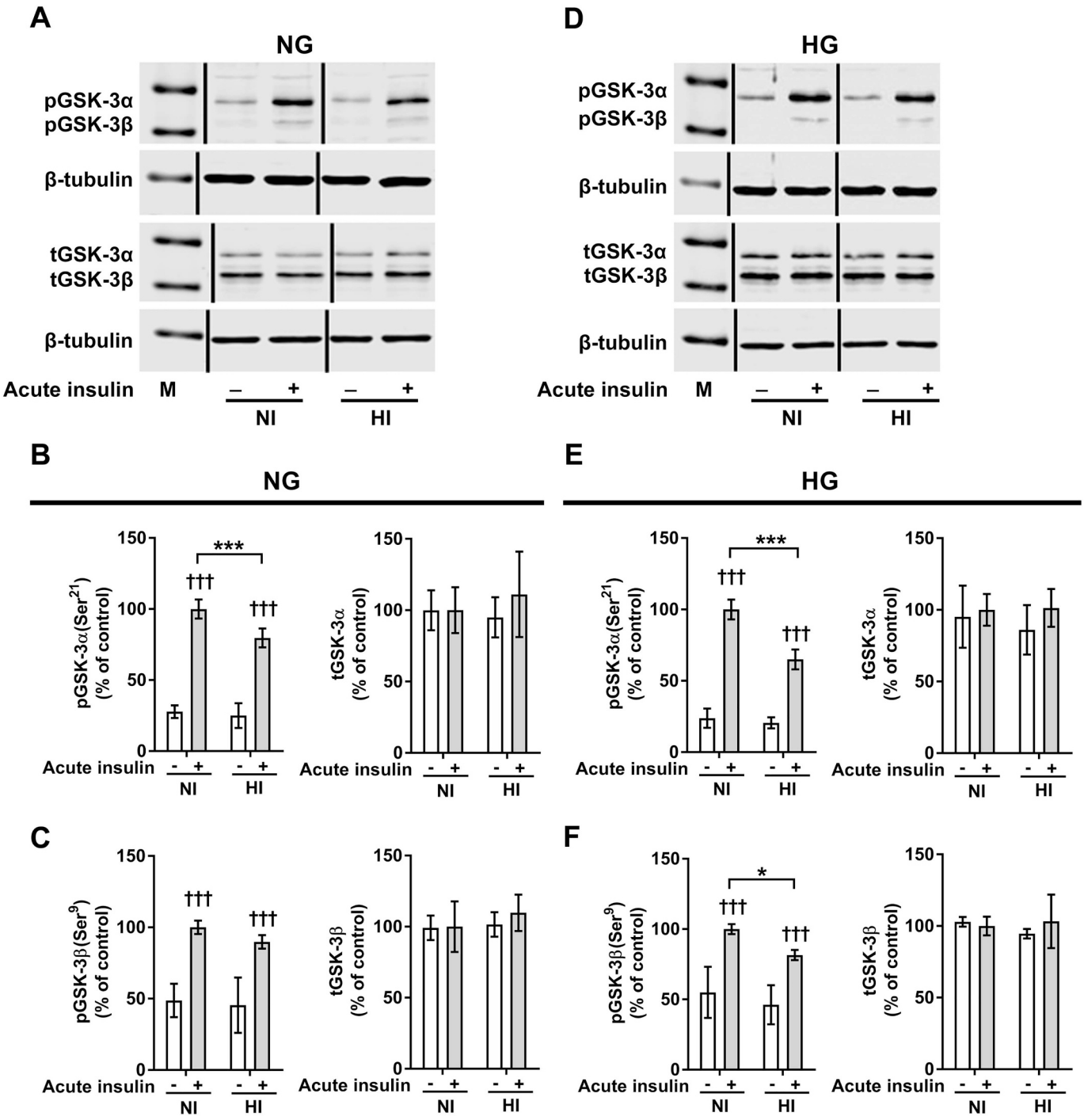

Fig. 3. Hyperinsulinemia impairs GSK-3 phosphorylation in VIC.
GSK-3α/β (Ser^{21}/Ser^{9}) phosphorylation of VIC cultured under hyperinsulinemia in normoglycemic (A-C) and hyperglycemic conditions is measured (D-F). Representative Western blot images show pGSK-3α/β (Ser^{21}/Ser^{9}) and respective levels of tGSK-3α/β protein expression (A/D). Density analysis was performed for quantification of pGSK-3α/β (Ser^{21}/Ser^{9}) and tGSK-3α/β signals under normoglycemic (B/C) and under hyperglycemic conditions (E/F). Data were normalized to β-tubulin and expressed relative to control with acute insulin stimulus. Experiments were performed with VIC derived from $n = 6$ individual sheep. NG: normoglycemia; HG: hyperglycemia; NI: normoinsulinemia; HI: hyperinsulinemia; M: marker; *: p-values < 0.05 between indicated groups; †: p-values < 0.05 compared to the according basal condition without acute insulin stimulus. Lanes of protein ladder represent 43 kDa and 55 kDa (tGSK and pGSK) and 55 kDa (β-tubulin). Vertical black lines in A and D indicate non-adjacent bands which have been cropped since there has been an additional treatment in between non-essential to this work.

mitochondrial function were examined in living cells. In VIC cultured under hyperinsulinemia with normoglycemic conditions, basal and glycolytic proton exchange rates increased by 57% ($p < 0.001$), and 50% ($p < 0.001$), respectively. Furthermore, hyperglycemia caused an increase in these parameters by 40% ($p < 0.01$), and 32% ($p < 0.05$), respectively. There was no additional effect of hyperinsulinemia in cells cultured under hyperglycemia (Fig. 5A/B). The injection of insulin during the glycolytic rate assay further enhanced the glycolytic proton exchange rates by 1.3-fold, both in cells cultured under normoglycemia ($p < 0.05$) and hyperglycemia ($p < 0.01$; Fig. 5 C). There was no effect of acute insulin treatment when hyperinsulinemia was present, indicating resistance to the effects of insulin on glucose oxidation. After

A

Tissue	GLUT1	GLUT2	GLUT4
Liver	Yes	Yes	No
Myocardium	Yes	No	Yes
Aortic valve	Yes	No	No

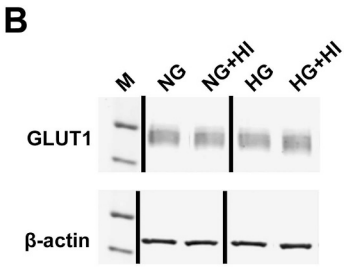

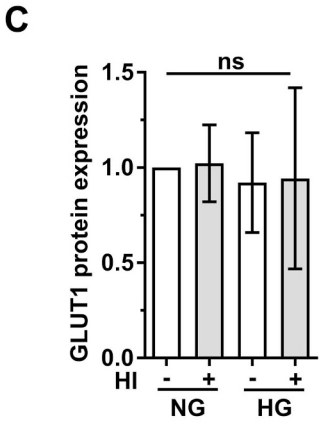

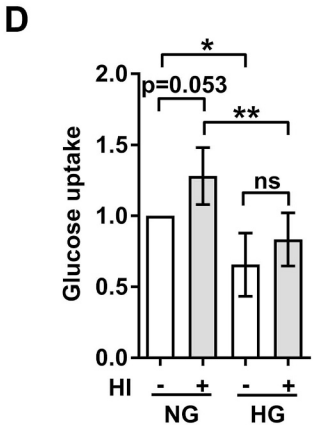

Fig. 4. GLUT1 expression and glucose uptake in VIC. Expression of GLUT1, GLUT2 and GLUT4 was analyzed in ovine liver, myocardium and aortic valve leaflets on mRNA level as well as GLUT1 on protein level. Aortic valve leaflets exclusively express GLUT1 (A). In cultured VIC, hyperinsulinemia and hyperglycemia treatment has no impact on GLUT1 protein expression (B/C). Western blot signals (B) are normalized to β-actin and expressed as values relative to control (C). Glucose uptake under normoglycemia is significantly enhanced by hyperinsulinemia, whereas this effect is abolished under hyperglycemia (D). Experiments were performed with VIC derived from $n = 6$ individual sheep. GLUT: glucose transporter; M: marker; NG: normoglycemia; HG; hyperglycemia; HI: hyperinsulinemia; *: $p < 0.05$; **: $p < 0.01$; ns: not significant. Lanes of protein ladder represent 43 kDa and 55 kDa.

assessing basal glycolytic rates, the cells were injected with rotenone and antimycin A to inhibit the respiratory chain (Fig. 5 D). Consequently, the cultures become fully dependent on glycolysis for ATP production. As seen in Fig. 5 D, compensatory glycolysis in VIC cultured under hyperinsulinemia was increased by 65% ($p < 0.001$). Hyperglycemia led to an increase under normoinsulinemia by 36% ($p < 0.01$), respectively versus normoglycemia. Hyperinsulinemia in cells cultured under hyperglycemia decreased compensatory glycolysis by 20% (Fig. 5 D).

Mitochondrial function was measured using the Seahorse XF Cell Mito Stress Test Kit. When VIC were cultured under hyperinsulinemia with normoglycemic conditions, basal mitochondrial respiration was increased by 2.0-fold ($p < 0.001$). A comparable 2.1-fold increase in basal mitochondrial respiration was observed under hyperglycemic conditions ($p < 0.001$) versus cells kept under normoglycemia. Culture under conditions combining hyperglycemia with chronic hyperinsulinemia led to a decrease in basal respiration by 21% ($p < 0.05$; Fig. 6 A). Subsequently, ATP production was calculated from the change in oxygen consumption rates after the injection of the ATP synthase/complex V inhibitor oligomycin. In line with the data obtained for basal mitochondrial respiration, ATP production was increased by 2.0- and 2.2-fold in cells cultured under hyperinsulinemia or hyperglycemia, respectively versus cells kept under normoglycemia (both $p < 0.001$). There was no additional effect on ATP production when hyperinsulinemia was combined with hyperglycemia (Fig. 6 B). Maximal respiration was determined from the changes in oxygen consumption rates after injection of the uncoupling agent carbonyl cyanide-4-(trifluoromethoxy)phenylhydrazone (FCCP). VIC cultured under hyperinsulinemia or hyperglycemia displayed a 3.1- and 2.2-fold higher maximal respiration, respectively versus cells kept under normoglycemia (both $p < 0.001$). The combination of hyperinsulinemia and hyperglycemia had no additional effect as compared to hyperinsulinemia or hyperglycemia alone (Fig. 6 C). The spare respiratory capacity compares maximal respiration with basal mitochondrial respiration. As shown in Fig. 6 D, both hyperinsulinemia and hyperglycemia promote a 25-fold ($p < 0.001$) and an 18-fold ($p < 0.05$) increase in spare respiratory capacity versus VIC cultured under normoglycemia. The combination of hyperglycemia and hyperinsulinemia did not elicit a statistically significant change in spare respiratory capacity.

3.7. Impact of hyperinsulinemia and hyperglycemia on key biological features of VIC in vitro

Finally we analyzed the impact of hyperinsulinemia and hyperglycemia on differentiation of VIC, extracellular matrix remodeling and osteogenic transformation of the cells. Upon phase contrast imaging an analysis of cultured VIC showed no obvious morphological difference by the applied treatments (Fig. 7 A). VIC grown on glass cover slips in lower cell count were stained with antibodies against vimentin and α-smooth muscle actin to visualize the activation state of cells due to the treatments (Fig. 7 B). Here, VIC expressed variable amounts of α-smooth muscle actin with no apparent difference in the amount of activated cells. However, on the level of gene expression hyperinsulinemia with or without additional hyperglycemia led to significant changes of α-smooth muscle actin (ACTA2) and collagen type 1 (COL1A1). ACTA2 expression was significantly downregulated by hyperinsulinemia ($p < 0.01$) as well as by the combination of hyperinsulinemia and hyperglycemia ($p < 0.05$; Fig. 7 C), whereas COL1A1 expression was significantly upregulated by the combination of both stimuli ($p < 0.05$; Fig. 7 C). Osteopontin (SPP1) gene expression, in contrast, was not influenced by the treatments (Fig. C). Further detection of calcium content also showed no effect (Fig. 7 D).

4. Discussion

4.1. Insulin sensitivity in VIC

It is known that endothelial cells are able to transport insulin into subendothelial tissue [24] and that diabetes leads to endothelial dysfunction in cardiovascular diseases (reviewed in [25]). Valvular endothelial cells and VIC are known to communicate with each other in the context of aortic valve degeneration [26]. Nevertheless, knowledge about cell type specific impact of diabetes in valvular diseases is scarce.

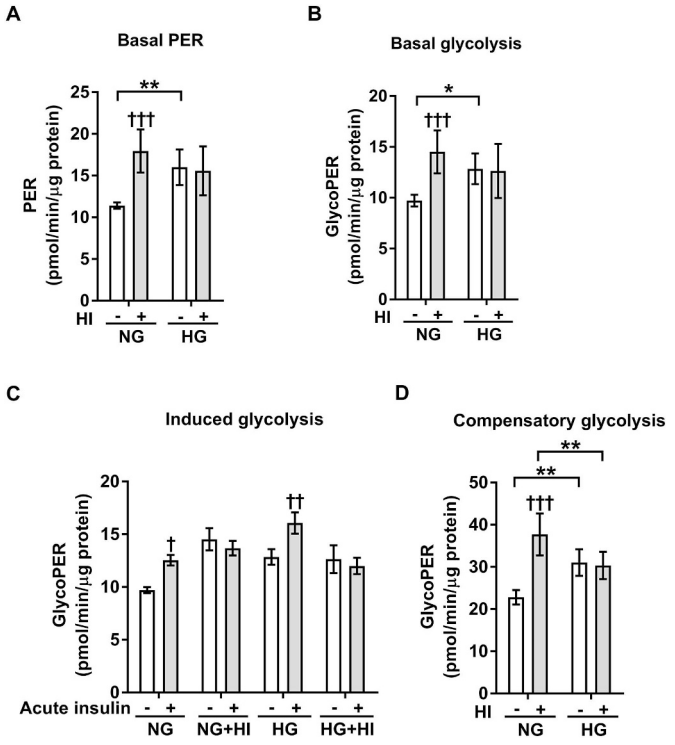

Fig. 5. Glycolytic rate assay.
VIC cultured under normo- and hyperglycemic conditions with or without hyperinsulinemia for five days were measured with a glycolytic rate assay using a Seahorse XFe96 extracellular flux analyzer. Basal (A) and glycolytic proton exchange rates (B) are increased by hyperinsulinemia under normoglycemia as well as under basal conditions by hyperglycemic treatment. Acute insulin stimulus leads to increased glycolytic proton exchange rates under normo- and hyperglycemic conditions, whereas hyperinsulinemia abolishes this effect (C). Analysis of compensatory glycolysis shows an increase of glycolytic proton exchange rates under normoglycemic conditions (D), as well as under hyperglycemic conditions with and without hyperinsulinemia. Experiments were performed with VIC derived from $n = 6$ individual sheep. PER: proton exchange rate; GlycoPER: glycolytic proton exchange rate; NG: normoglycemia; HG: hyperglycemia; HI: hyperinsulinemia; *: p-values < 0.05 between indicated groups; †: p-values < 0.05 compared to the according basal condition without hyperinsulinemia or acute insulin stimulus, respectively; *: $p < 0.05$; **: $p < 0.01$; †: $p < 0.05$; ††: $p < 0.01$; †††: $p < 0.001$.

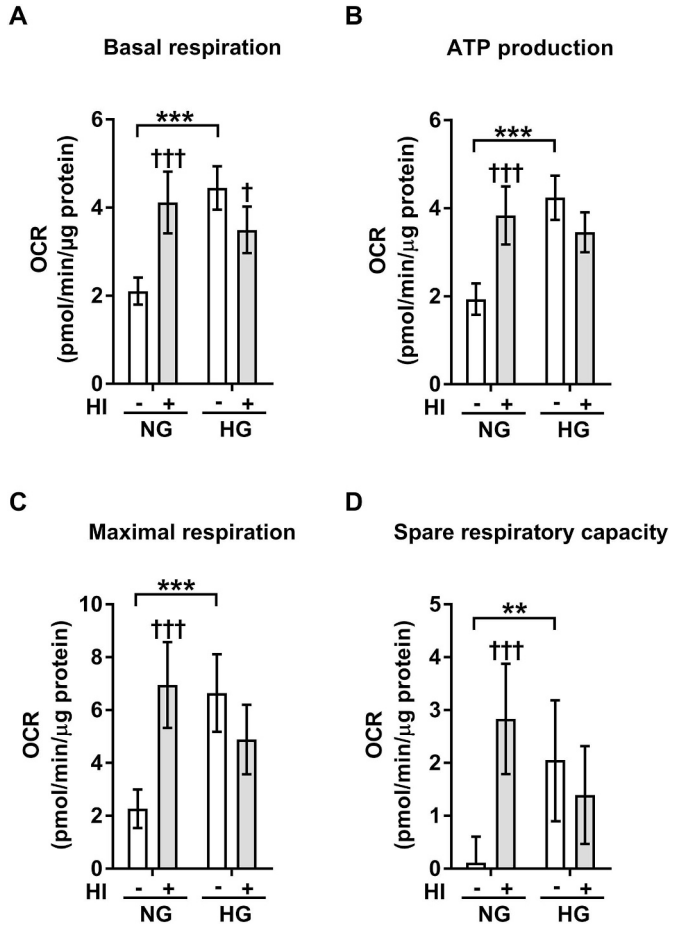

Fig. 6. Mitochondrial stress assay.
VIC cultured for five days under normo- and hyperglycemic conditions with or without hyperinsulinemia were measured with a mitochondrial stress assay using a Seahorse XFe96 extracellular flux analyzer. Basal respiration (A), ATP production (B), maximal respiration (C) and spare respiratory capacity (D) were significantly enhanced by hyperinsulinemia under normoglycemia as well as under basal conditions by hyperglycemic treatment. Experiments were performed with VIC derived from $n = 6$ individual sheep. OCR: oxygen consumption rate; NG: normoglycemia; HG: hyperglycemia; HI: hyperinsulinemia; *: p-values < 0.05 between indicated groups; †: p-values < 0.05 compared to the according basal condition without hyperinsulinemia; **: $p < 0.01$; ***: $p < 0.001$; †: $p < 0.05$; †††: $p < 0.001$.

In this work we focused on VIC as the quantitatively major cell type of the aortic valve.

In detail, we concentrated on the impact of hyperinsulinemia and hyperglycemia on VIC. Our study shows that VIC are sensitive to insulin and hyperglycemia, respectively, indicating a direct impact of diabetes on the heart valve itself.

We analyzed the impact of insulin on VIC proliferation, since it has been shown that vascular smooth muscle cells and pericytes have increased proliferative properties when exposed to chronic insulin stimulation [27,28]. In the present study VIC showed an increase in proliferation under hyperinsulinemia in normoglycemic conditions. Increase of proliferation by hyperglycemia alone or in combination with chronic insulin as previously described for vascular smooth muscle cells [29,30] was not present in VIC. The opposite effect, i.e. decreased proliferation has been described for skin fibroblasts treated with high glucose or derived from diabetic patients [31,32]. However, our findings suggest that hyperinsulinemia and not hyperglycemia is the main trigger for proliferation of VIC. It has been shown that VIC in sclerotic valves demonstrate a greater proliferative activity than cells in already calcified, i.e. stenotic valves [33]. In front of this background, increased proliferation due to hyperinsulinemia might be an early step towards heart valve sclerosis in pre-diabetes.

4.2. Insulin receptors in VIC

Insulin receptors are known to be expressed in vascular tissues and in vascular smooth muscle cells [34,35]. Our data provide further evidence on the mRNA expression of both insulin receptor and IGF1-receptor in VIC. However, expression of these receptors in VIC was not influenced by hyperinsulinemia, by hyperglycemia or by the combination of both. Reports on insulin-induced changes in the amount of the insulin receptor are controversial and seem to be cell type dependent [36,37]. Nevertheless, expression of IGF1-receptor has been shown to be increased in aortas from obesity-induced diabetic *db/db* mice [38], indicating that not isolated hyperinsulinemia or hyperglycemia but rather the complex interplay of a metabolic phenotype might be the driving force.

4.3. Impaired Akt- and GSK-3α/β-phosphorylation in VIC under hyperinsulinemia and hyperglycemia

Increased Akt phosphorylation after acute insulin stimulation shows insulin sensitivity of VIC. A study on cardiac fibroblasts also reported

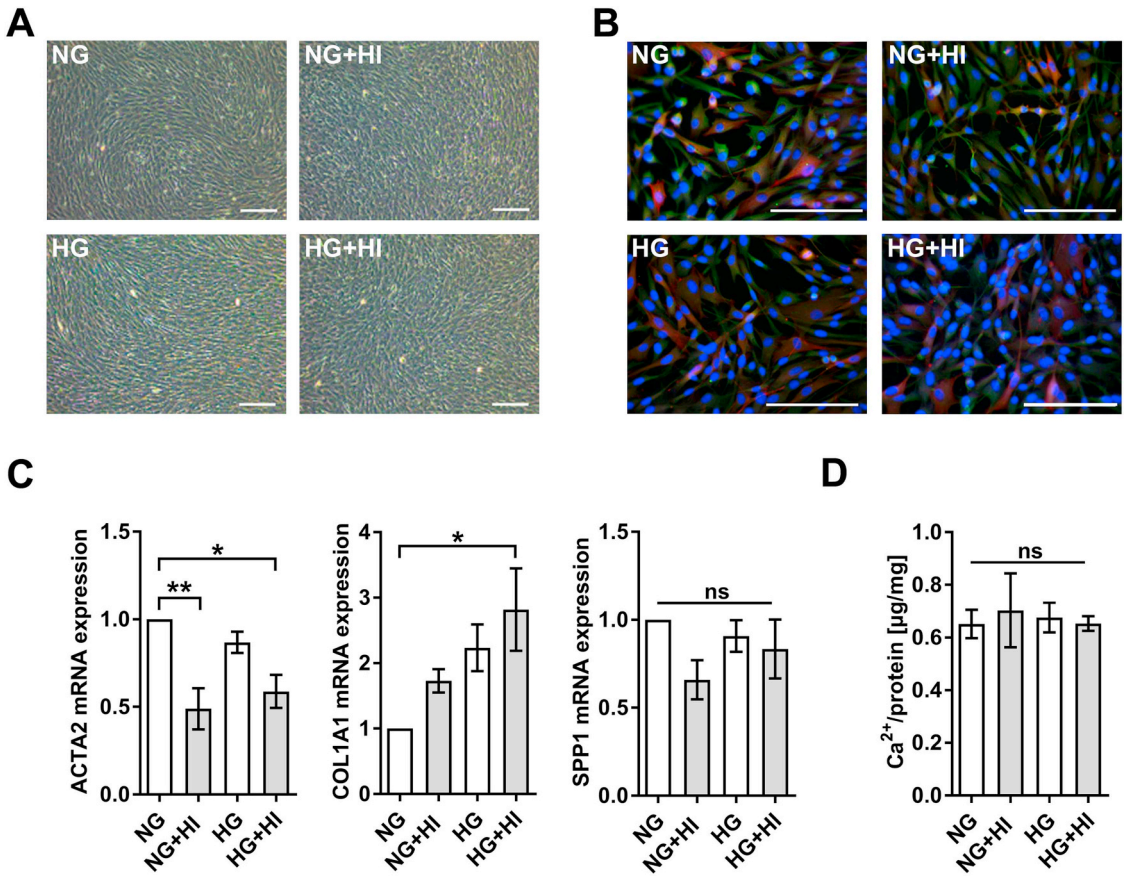

Fig. 7. Impact of hyperinsulinemia and hyperglycemia on VIC in vitro.
Hyperinsulinemia and hyperglycemia are capable of modulating key biological features of VIC in vitro. Morphology of cultured VIC remains unaltered when treated with hyperinsulinemia, hyperglycemia or the combination of both as detected by light microscopy (A). Immunohistological images with antibodies against vimentin (green) and α-smooth muscle actin (red) showing the presence of activated VIC (B). Gene expression analysis revealed significantly lower expression of ACTA2 in VIC under hyperinsulinemia with or without hyperglycemia, whereas COL1A1 was upregulated by the combination of hyperglycemia and hyperinsulinemia. Gene expression of SPP1 remained unaltered (C). Under the applied *in vitro* conditions there were no significant differences in the calcium content of VIC (D). Experiments were performed with VIC derived from $n = 6$ individual sheep. ACTA2: α-smooth muscle actin; COL1A1: collagen type 1; SPP1: osteopontin; NG: normoglycemia; HG: hyperglycemia; HI: hyperinsulinemia; *: $p < 0.05$; **: $p < 0.01$; ns: not significant; bars: 200 µm (A), 100 µm (B).

Akt phosphorylation by acute insulin, but with remarkably lower phosphorylation levels as compared to those levels observed here in VIC [39]. Impaired insulin signaling in cardiomyocytes has been previously shown [40–42]. However, the impact of diabetes on classical insulin signaling in cardiac valvular cells remains unknown to date. Our analyses of insulin receptor signaling show that even short time incubation of VIC for five days under hyperinsulinemia and hyperglycemia is sufficient to evoke a considerably impaired insulin response in these cells as indicated by decreased phosphorylation of Akt and GSK-3α/β. Interestingly, isolated hyperinsulinemia under normoglycemia already leads to an impaired insulin action. Phosphorylation of Akt induced by hyperglycemia alone as we have seen in VIC has also been reported for cardiomyocytes in a recent publication [43]. In contrast, cardiac fibroblasts from patients with type 2 diabetes showed no regulation in Akt phosphorylation at all when compared with cardiac fibroblasts from non-diabetics [44], which might be due to the cultivation of the isolated cells under non-diabetic conditions after isolation. This might be indicative for the reversible capacities of cardiovascular cells.

4.4. Glucose transporters

Our analyses show that VIC solely express GLUT1, whereas GLUT4, which has been described to be expressed in cardiomyocytes already in the 1990s [45,46], is not present in VIC. Besides numerous reports on GLUT4 expression in cardiac muscle (reviewed in [47]) or in fibroblasts differentiating into adipocytes (reviewed in [48]), reports on GLUT4 expression in undifferentiated fibroblasts or cardiac fibroblasts are rare [49,50]. Since we have shown that VIC are highly responsive to insulin but do not express GLUT4, we also analyzed whether the expression of GLUT1 is altered by hyperinsulinemia or hyperglycemia. Changes in GLUT1 expression due to hyperinsulinemia have been reported *in vivo* and *in vitro* before [45,51,52]. However, in VIC GLUT1 was not altered by hyperglycemia or hyperinsulinemia. This effect in the above mentioned reports might be attributed to a regulation of GLUT1 expression in dependence of the concurrent interference of GLUT4 which is non-existent in VIC. Alternatively, unchanged GLUT1 expression in VIC might be due to the lack of additional stimulators, e.g. such as changes in hormone balance [53] or disturbed fatty acid metabolism [54], which are present in other diabetic tissues or cells therefrom. Finally, it cannot be excluded that there are other GLUT forms present in VIC which are not yet characterized in detail and which might act in a compensatory way thus leading to an unchanged GLUT1 expression. Although GLUT have high sequence identity and are highly conserved amongst different species [55], e.g. GLUT11 has been shown to be absent in rats and mice [56].

4.5. Glucose uptake in VIC

In VIC, hyperglycemia alone led to a decreased glucose uptake, which has also been reported for smooth muscle cells and

cardiomyocytes before [57,58]. The combination of hyperinsulinemia and hyperglycemia did not show a significant decrease in glucose uptake in VIC, which is contrary to previous findings in other tissues, i.e. in lymphatic muscle cells. Here, the combination of these both stimuli leads to a decreased glucose uptake of the cells [59]. Interestingly, cardiac fibroblasts also do not show an effect regarding glucose uptake under such a combined treatment or under hyperglycemia alone [39]. Analyses of kinetics show that GLUT1 has a high affinity to glucose and a low Km value in comparison to GLUT2 and 4 (reviewed by [60]). Moreover, glucose uptake by GLUT1 has been shown to reach a maximum, or a plateau phase, respectively [61]. Although such detailed analysis of glucose uptake for individual GLUT has not been reported for myocardial or valvular cells, the aforementioned observations might explain the unchanged glucose uptake even with higher concentrations of glucose. Surprisingly, hyperinsulinemia under normoglycemic conditions led to a nearly significant increase in glucose uptake in VIC. This cannot be explained by an increase of GLUT1 expression which remains unaltered in VIC under either treatment. Our data thus may provide the first evidence that VIC are susceptible to hyperinsulinemia alone in developing a disturbed insulin signaling. However, this stimulus appears to be not strong enough to disturb glucose uptake under additional hyperglycemic conditions.

4.6. Glycolysis and mitochondrial respiration in VIC

Hyperinsulinemia in front of a normoglycemic background or hyperglycemia alone led to increased basal proton exchange rates and therefore to enhanced basal glycolysis as well as to increased compensatory glycolysis. The combination of hyperglycemia and hyperinsulinemia abolished this effect. Induced glycolysis showed that only VIC without prior chronic exposure to insulin reacted with an increase to an acute insulin stimulus. Analysis of mitochondrial respiration showed that similarly to results of glycolytic function, VIC showed an increase in basal and maximal respiration under normoglycemic hyperinsulinemia and under hyperglycemia alone. Moreover, these conditions also led to an increased ATP production and to an increased spare respiratory capacity.

Our Seahorse data suggest that in contrast to energy-dependent or classical insulin-dependent tissue, VIC are not impaired in their glycolytic and thus mitochondrial function when the cells are exposed to diabetic conditions. Direct correlation between insulin-resistance and impaired metabolism in this context has been shown in several tissues and cells like lymphatic muscle cells [59], vascular cells [62] as well as in skeletal muscle [63] and adipose tissue [64].

VIC do not express GLUT4 and thus do not follow the classical insulin pathway beginning at impaired insulin sensitivity leading necessarily to impaired glucose uptake and finally resulting in disturbed bioenergetics. Enhanced metabolic activities by conditions which coincidentally lead to impaired insulin sensitivity are a mechanism by which VIC may be directed towards unregulated proliferation and differentiation. This in turn may then promote fibrotic changes and trigger early pathogenesis of heart valve degeneration.

4.7. Impact of hyperinsulinemia and hyperglycemia on degenerative processes in VIC

Degenerative processes in aortic heart valves are accompanied by disturbed extra cellular matrix assembly, inflammation, lipid accumulation and finally calcification [65,66]. Early phases of degenerative processes in aortic valves are characterized by thickening of the valve leaflet due to increased extracellular matrix synthesis [67], as we have recently shown for the proteoglycan biglycan [68]. Moreover, differentiation of quiescent VIC towards a myofibroblastoidal phenotype in degenerative processes has been reported [69], whereas the appearance of α-smooth muscle actin-positive cells in early lesions of valves was rare [70]. Nevertheless, knowledge about the impact of diabetes on early phases of aortic valve degeneration is limited, whereas it is known that fibrosis and changes in extracellular matrix components like collagen is aggravated in cardiovascular tissues of diabetics [71–73].

Our studies demonstrate that hyperinsulinemia and hyperglycemia do not alter the macroscopic phenotype of VIC. Moreover, osteopontin expression and *in vitro* calcium deposition is not altered, indicating that our treatment was not yet sufficient to provoke hallmarks of late stage degeneration, i.e. calcification, whereas further observations may point to early stages of degenerative changes.

Hyperglycemia alone did not alter α-smooth muscle actin or collagen type 1 gene expression. This is somewhat surprising, since in other cell types (i.e. cardiac fibroblasts) several publications have reported an enhanced proliferation, together with increased α-smooth muscle actin and collagen expression [74–77]. However, a recent study of Gorski and colleagues [39] has shown no upregulation of collagen and α-smooth muscle actin in cardiac fibroblasts by hyperglycemia alone [39].

Nevertheless, our study shows that a combination of hyperinsulinemia and hyperglycemia leads to an upregulation of collagen type 1 gene expression, resembling the findings of Gorski et al. on cardiac fibroblasts derived from diabetic mice. This indicates that hyperinsulinemia rather than hyperglycemia may be the driving force for early fibrotic changes in VIC. Surprisingly, hyperinsulinemia generally led to a decrease in α-smooth muscle actin gene expression in VIC. Cardiac fibroblasts derived from diabetic mice treated with hyperglycemia subsequently, in contrast display an increase in α-smooth muscle actin gene expression [39]. We speculate that these differences between our observations and findings of the latter study may be related to the lack of further diabetic characteristics such as inflammation and the involvement of the immune system in our VIC *in vitro* system.

4.8. Conclusion

VIC are susceptible to insulin by expressing insulin receptors and increasing proliferation activity under hyperinsulinemia. Under the conditions of hyperinsulinemia or hyperglycemia VIC develop an impaired insulin response. Simultaneously, glucose uptake of VIC was increased under hyperinsulinemia, while it was impaired under hyperglycemia. Glycolytic capacity and mitochondrial function are not decreased but in contrast are activated by these stimuli, indicating that diabetic conditions lead to impaired insulin signaling in combination with exaggerated metabolic activity. Hyperinsulinemia in combination with hyperglycemia leads to pro-fibrotic changes in VIC, though yet without features of late stage disease, e.g. osteogenic differentiation or calcification. These findings suggest hyperinsulinemia and hyperglycemia as possible factors in early phases of the development of heart valve degeneration.

Funding

This work was supported by the German Heart Foundation/German Foundation of Heart Research to M.B. (Dr. Rusche Research Project 2016).

Data statement

Primary data and datasets used and/or analyzed during the current study are available from the corresponding author on reasonable request.

Transparency document

The Transparency document associated with this article can be found, in online version.

Declaration of Competing Interest

Parts of the herein presented data have been demonstrated on the occasion of the annual meeting of the German Society of Thoracic- and Cardiovascular Surgery (DGTHG) and European Association for the Study of Diabetes (EASD).

Acknowledgements

The authors thank Neslihan Odabasi for excellent technical assistance. The generous support of the S. Bunnenberg Foundation to the Cardiovascular Research Facilities at the Heinrich-Heine-University Düsseldorf is greatly appreciated. This work was supported by the German Research Foundation (SFB1116).

References

[1] E. Ginter, V. Simko, Type 2 diabetes mellitus, pandemic in 21st century, Adv. Exp. Med. Biol. 771 (2012) 42–50.
[2] C.S. Fox, S.H. Golden, C. Anderson, et al., Update on prevention of cardiovascular disease in adults with type 2 diabetes mellitus in light of recent evidence: a scientific statement from the American Heart Association and the American Diabetes Association, Circulation 132 (2015) 691–718, https://doi.org/10.1161/CIR.0000000000000230.
[3] C.C. Low Wang, C.N. Hess, W.R. Hiatt, et al., Clinical update: cardiovascular disease in diabetes mellitus: atherosclerotic cardiovascular disease and heart failure in type 2 diabetes mellitus - mechanisms, management, and clinical considerations, Circulation 133 (2016) 2459–2502, https://doi.org/10.1161/CIRCULATIONAHA.116.022194.
[4] S. Gray, J.K. Kim, New insights into insulin resistance in the diabetic heart, Trends Endocrinol. Metab. 22 (2011) 394–403, https://doi.org/10.1016/j.tem.2011.05.001.
[5] Kitada M, Zhang Z, Mima A, et al. Molecular mechanisms of diabetic vascular complications. *J Diabetes Investig* 2010; 1: 77–89. 2010/06/01. DOI: https://doi.org/10.1111/j.2040-1124.2010.00018.x.
[6] Einarson TR, Acs A, Ludwig C, et al. Prevalence of cardiovascular disease in type 2 diabetes: a systematic literature review of scientific evidence from across the world in 2007–2017. *Cardiovasc Diabetol* 2018; 17: 83. 2018/06/10. DOI: https://doi.org/10.1186/s12933-018-0728-6.
[7] K. Eguchi, B. Boden-Albala, Z. Jin, et al., Association between diabetes mellitus and left ventricular hypertrophy in a multiethnic population, Am. J. Cardiol. 101 (2008) 1787–1791, https://doi.org/10.1016/j.amjcard.2008.02.082.
[8] D.S. Bell, Heart failure: the frequent, forgotten, and often fatal complication of diabetes, Diabetes Care 26 (2003) 2433–2441.
[9] J.K. Boyer, S. Thanigaraj, K.B. Schechtman, et al., Prevalence of ventricular diastolic dysfunction in asymptomatic, normotensive patients with diabetes mellitus, Am. J. Cardiol. 93 (2004) 870–875, https://doi.org/10.1016/j.amjcard.2003.12.026.
[10] H. Taegtmeyer, J.M. Passmore, Defective energy metabolism of the heart in diabetes, Lancet 1 (1985) 139–141.
[11] P. Iozzo, P. Chareonthaitawee, D. Dutka, et al., Independent association of type 2 diabetes and coronary artery disease with myocardial insulin resistance, Diabetes 51 (2002) 3020–3024.
[12] L.A. Barouch, D. Gao, L. Chen, et al., Cardiac myocyte apoptosis is associated with increased DNA damage and decreased survival in murine models of obesity, Circ. Res. 98 (2006) 119–124, https://doi.org/10.1161/01.RES.0000199348.10580.1d.
[13] Y. Hinokio, S. Suzuki, M. Hirai, et al., Oxidative DNA damage in diabetes mellitus: its association with diabetic complications, Diabetologia 42 (1999) 995–998, https://doi.org/10.1007/s001250051258.
[14] K. Le Quang, R. Bouchareb, D. Lachance, et al., Early development of calcific aortic valve disease and left ventricular hypertrophy in a mouse model of combined dyslipidemia and type 2 diabetes mellitus, Arterioscler. Thromb. Vasc. Biol. 34 (2014) 2283–2291, https://doi.org/10.1161/ATVBAHA.114.304205.
[15] A.T. Yan, M. Koh, K.K. Chan, et al., Association between cardiovascular risk factors and aortic stenosis, The CANHEART Aortic Stenosis Study. *J Am Coll Cardiol* 69 (2017) 1523–1532, https://doi.org/10.1016/j.jacc.2017.01.025.
[16] S.C. Larsson, A. Wallin, N. Hakansson, et al., Type 1 and type 2 diabetes mellitus and incidence of seven cardiovascular diseases, Int. J. Cardiol. 262 (2018) 66–70, https://doi.org/10.1016/j.ijcard.2018.03.099.
[17] J. Ljungberg, B. Johansson, K.G. Engstrom, et al., Traditional cardiovascular risk factors and their relation to future surgery for valvular heart disease or ascending aortic disease: a case-referent study, J. Am. Heart Assoc. 6 (2017), https://doi.org/10.1161/JAHA.116.005133.
[18] Y. Huang, X. Cai, W. Mai, et al., Association between prediabetes and risk of cardiovascular disease and all cause mortality: systematic review and meta-analysis, BMJ 355 (2016) i5953, , https://doi.org/10.1136/bmj.i5953.
[19] Gross L and Kugel MA. Topographic Anatomy and Histology of the Valves in the Human Heart. *Am J Pathol* 1931; 7: 445-474 447. 1931/09/01.
[20] Filip DA, Radu A and Simionescu M. Interstitial cells of the heart valves possess characteristics similar to smooth muscle cells. *Circ Res* 1986; 59: 310–320. 1986/09/01.
[21] A. Rutkovskiy, A. Malashicheva, G. Sullivan, et al., Valve interstitial cells: the key to understanding the pathophysiology of heart valve calcification, J. Am. Heart Assoc. 6 (2017), https://doi.org/10.1161/JAHA.117.006339.
[22] N. Romero, P. Swain, A. Neilson, et al., Improving Quantification of Cellular Glycolytic Rate Using Agilent Seahorse XF Technology (White Paper), Agilent Technologies, Inc, 2017 (5991-7894EN).
[23] J. Boucher, A. Kleinridders, C.R. Kahn, Insulin receptor signaling in normal and insulin-resistant states, Cold Spring Harb. Perspect. Biol. 6 (2014), https://doi.org/10.1101/cshperspect.a009191.
[24] King GL and Johnson SM. Receptor-mediated transport of insulin across endothelial cells. *Science* 1985; 227: 1583–1586. 1985/03/29.
[25] Roberts AC and Porter KE. Cellular and molecular mechanisms of endothelial dysfunction in diabetes. Diab. Vasc. Dis. Res. 2013; 10: 472-482. 2013/09/05. DOI: https://doi.org/10.1177/1479164113500680.
[26] Hjortnaes J, Shapero K, Goettsch C, et al. Valvular interstitial cells suppress calcification of valvular endothelial cells. *Atherosclerosis* 2015; 242: 251–260. 2015/08/02. DOI: https://doi.org/10.1016/j.atherosclerosis.2015.07.008.
[27] Nagai M, Kamide K, Rakugi H, et al. Role of endothelin-1 induced by insulin in the regulation of vascular cell growth. *Am J Hypertens* 2003; 16: 223–228. 2003/03/07.
[28] Schneider DJ, Absher PM and Ricci MA. Dependence of augmentation of arterial endothelial cell expression of plasminogen activator inhibitor type 1 by insulin on soluble factors released from vascular smooth muscle cells. *Circulation* 1997; 96: 2868–2876. 1997/12/31.
[29] Fujita N, Furukawa Y, Du J, et al. Hyperglycemia enhances VSMC proliferation with NF-kappaB activation by angiotensin II and E2F-1 augmentation by growth factors. *Mol Cell Endocrinol* 2002; 192: 75–84. 2002/06/29.
[30] Cersosimo E, Xu X, Upala S, et al. Acute insulin resistance stimulates and insulin sensitization attenuates vascular smooth muscle cell migration and proliferation. Physiol Rep 2014; 2 2014/08/21. DOI: 10.14814/phy2.12123.
[31] Loots MA, Lamme EN, Mekkes JR, et al. Cultured fibroblasts from chronic diabetic wounds on the lower extremity (non-insulin-dependent diabetes mellitus) show disturbed proliferation. *Arch Dermatol Res* 1999; 291: 93–99. 1999/04/09.
[32] Hehenberger K, Heilborn JD, Brismar K, et al. Inhibited proliferation of fibroblasts derived from chronic diabetic wounds and normal dermal fibroblasts treated with high glucose is associated with increased formation of l-lactate. *Wound Repair Regen* 1998; 6: 135–141. 1998/10/20.
[33] Tuleta I, Al Ghaddioui AK, Bauriedel G, et al. The imbalance between proliferation and apoptosis contributes to degeneration of aortic valves and bioprostheses. *Cardiol J* 2013; 20: 268–276. 2013/06/22. DOI: https://doi.org/10.5603/CJ.2013.0072.
[34] Jialal I, Crettaz M, Hachiya HL, et al. Characterization of the receptors for insulin and the insulin-like growth factors on micro- and macrovascular tissues. Endocrinology 1985; 117: 1222-1229. 1985/09/01. DOI: https://doi.org/10.1210/endo-117-3-1222.
[35] Johansson GS and Arnqvist HJ. Insulin and IGF-I action on insulin receptors, IGF-I receptors, and hybrid insulin/IGF-I receptors in vascular smooth muscle cells. Am. J. Physiol. Endocrinol. Metab. 2006; 291: E1124-1130. 2006/06/29. DOI: https://doi.org/10.1152/ajpendo.00565.2005.
[36] Catalano KJ, Maddux BA, Szary J, et al. Insulin resistance induced by hyperinsulinemia coincides with a persistent alteration at the insulin receptor tyrosine kinase domain. PLoS One 2014; 9: e108693. 2014/09/27. DOI: https://doi.org/10.1371/journal.pone.0108693.
[37] Gavin JR, 3rd, Roth J, Neville DM, Jr., et al. Insulin-dependent regulation of insulin receptor concentrations: a direct demonstration in cell culture. *Proc Natl Acad Sci U S A* 1974; 71: 84–88. 1974/01/01.
[38] Engberding N, San Martin A, Martin-Garrido A, et al. Insulin-like growth factor-1 receptor expression masks the antiinflammatory and glucose uptake capacity of insulin in vascular smooth muscle cells. *Arterioscler Thromb Vasc Biol* 2009; 29: 408–415. 2009/01/06. DOI: https://doi.org/10.1161/ATVBAHA.108.181727.
[39] Gorski DJ, Petz A, Reichert C, et al. Cardiac fibroblast activation and hyaluronan synthesis in response to hyperglycemia and diet-induced insulin resistance. Sci. Rep. 2019; 9: 1827. 2019/02/14. DOI: https://doi.org/10.1038/s41598-018-36140-6.
[40] Morisco C, Lembo G and Trimarco B. Insulin resistance and cardiovascular risk: New insights from molecular and cellular biology. *Trends Cardiovasc Med* 2006; 16: 183–188. 2006/07/15. DOI: https://doi.org/10.1016/j.tcm.2006.03.008.
[41] Fu Q, Wang Q and Xiang YK. Insulin and beta adrenergic receptor signaling: crosstalk in heart. Trends Endocrinol. Metab. 2017; 28: 416–427. 2017/03/04. DOI: https://doi.org/10.1016/j.tem.2017.02.002.
[42] Abel ED. Glucose transport in the heart. *Front Biosci* 2004; 9: 201–215. 2004/02/10.
[43] Su D, Zhou Y, Hu S, et al. Role of GAB1/PI3K/AKT signaling high glucose-induced cardiomyocyte apoptosis. Biomed. Pharmacother. 2017; 93: 1197-1204. 2017/07/26. DOI: https://doi.org/10.1016/j.biopha.2017.07.063.
[44] Sedgwick B, Riches K, Bageghni SA, et al. Investigating inherent functional differences between human cardiac fibroblasts cultured from nondiabetic and type 2 diabetic donors. Cardiovasc. Pathol. 2014; 23: 204-210. 2014/04/22. DOI: https://doi.org/10.1016/j.carpath.2014.03.004.
[45] Laybutt DR, Thompson AL, Cooney GJ, et al. Selective chronic regulation of GLUT1 and GLUT4 content by insulin, glucose, and lipid in rat cardiac muscle in vivo. Am. J. Phys. 1997; 273: H1309-1316. 1997/10/10. DOI: https://doi.org/10.1152/ajpheart.1997.273.3.H1309.
[46] Martin S, Rice JE, Gould GW, et al. The glucose transporter GLUT4 and the aminopeptidase vp165 colocalise in tubulo-vesicular elements in adipocytes and cardiomyocytes. *J Cell Sci* 1997; 110 (Pt 18): 2281–2291. 1997/10/24.
[47] Szablewski L. Glucose transporters in healthy heart and in cardiac disease. *Int J*

Cardiol 2017; 230: 70–75. 2016/12/31. DOI: https://doi.org/10.1016/j.ijcard.2016.12.083.
[48] Govers R. Molecular mechanisms of GLUT4 regulation in adipocytes. Diabetes Metab. 2014; 40: 400-410. 2014/03/25. DOI: https://doi.org/10.1016/j.diabet.2014.01.005.
[49] Longo N, Bell GI, Shuster RC, et al. Human fibroblasts express the insulin-responsive glucose transporter (GLUT4). *Trans Assoc Am Physicians* 1990; 103: 202–213. 1990/01/01.
[50] Prata C, Zambonin L, Rizzo B, et al. Glycosides from Stevia rebaudiana Bertoni possess insulin-mimetic and antioxidant activities in rat cardiac fibroblasts. Oxidative Med. Cell. Longev. 2017; 2017: 3724545. 2017/09/28. DOI: https://doi.org/10.1155/2017/3724545.
[51] Pryor PR, Liu SC, Clark AE, et al. Chronic insulin effects on insulin signalling and GLUT4 endocytosis are reversed by metformin. *Biochem J* 2000; 348 Pt 1: 83–91. 2000/05/05.
[52] de Laat MA, Clement CK, Sillence MN, et al. The impact of prolonged hyperinsulinaemia on glucose transport in equine skeletal muscle and digital lamellae. *Equine Vet J* 2015; 47: 494–501. 2014/07/06. DOI: https://doi.org/10.1111/evj.12320.
[53] Penicaud L, Leloup C, Fioramonti X, et al. Brain glucose sensing: a subtle mechanism. *Curr Opin Clin Nutr Metab Care* 2006; 9: 458–462. 2006/06/17. DOI: https://doi.org/10.1097/01.mco.0000232908.84483.e0.
[54] Lam TK, Pocai A, Gutierrez-Juarez R, et al. Hypothalamic sensing of circulating fatty acids is required for glucose homeostasis. *Nat Med* 2005; 11: 320–327. 2005/03/01. DOI: https://doi.org/10.1038/nm1201.
[55] Zhao FQ and Keating AF. Functional properties and genomics of glucose transporters. *Curr Genomics* 2007; 8: 113–128. 2008/07/29.
[56] Scheepers A, Schmidt S, Manolescu A, et al. Characterization of the human SLC2A11 (GLUT11) gene: alternative promoter usage, function, expression, and subcellular distribution of three isoforms, and lack of mouse orthologue. *Mol Membr Biol* 2005; 22: 339–351. 2005/09/13. DOI: https://doi.org/10.1080/09687860500166143.
[57] Davidoff AJ, Davidson MB, Carmody MW, et al. Diabetic cardiomyocyte dysfunction and myocyte insulin resistance: role of glucose-induced PKC activity. *Mol Cell Biochem* 2004; 262: 155–163. 2004/11/10.
[58] Kaiser N, Sasson S, Feener EP, et al. Differential regulation of glucose transport and transporters by glucose in vascular endothelial and smooth muscle cells. *Diabetes* 1993; 42: 80–89. 1993/01/01.
[59] Lee Y, Fluckey JD, Chakraborty S, et al. Hyperglycemia- and hyperinsulinemia-induced insulin resistance causes alterations in cellular bioenergetics and activation of inflammatory signaling in lymphatic muscle. *FASEB J* 2017; 31: 2744–2759. 2017/03/17. DOI: https://doi.org/10.1096/fj.201600887R.
[60] Wilcox G. Insulin and insulin resistance. *Clin Biochem Rev* 2005; 26: 19–39. 2005/11/10.
[61] H.B.A. Lodish, C.A. Kaiser, M. Krieger, A. Bretscher, H. Ploegh, A. Amon, K. Martin, Molecular Cell Biology, 8th ed, Macmillan Education, 2016.
[62] Merdzo I, Rutkai I, Tokes T, et al. The mitochondrial function of the cerebral vasculature in insulin-resistant Zucker obese rats. Am. J. Physiol. Heart Circ. Physiol. 2016; 310: H830-838. 2016/02/14. DOI: https://doi.org/10.1152/ajpheart.00964.2015.
[63] Kelley DE, He J, Menshikova EV, et al. Dysfunction of mitochondria in human skeletal muscle in type 2 diabetes. *Diabetes* 2002; 51: 2944–2950. 2002/09/28.
[64] Sen S, Domingues CC, Rouphael C, et al. Genetic modification of human mesenchymal stem cells helps to reduce adiposity and improve glucose tolerance in an obese diabetic mouse model. *Stem Cell Res Ther* 2015; 6: 242. 2015/12/15. DOI: https://doi.org/10.1186/s13287-015-0224-9.
[65] R.V. Freeman, C.M. Otto, Spectrum of calcific aortic valve disease: pathogenesis, disease progression, and treatment strategies, Circulation 111 (2005) 3316–3326, https://doi.org/10.1161/CIRCULATIONAHA.104.486738.
[66] Xu S and Grande-Allen KJ. The role of cell biology and leaflet remodeling in the progression of heart valve disease. *Methodist Debakey Cardiovasc J* 2010; 6: 2–7. 2010/04/03.
[67] J.H. Chen, C.A. Simmons, Cell-matrix interactions in the pathobiology of calcific aortic valve disease: critical roles for matricellular, matricrine, and matrix mechanics cues, Circ. Res. 108 (2011) 1510–1524, https://doi.org/10.1161/CIRCRESAHA.110.234237.
[68] Barth M, Selig JI, Klose S, et al. Degenerative aortic valve disease and diabetes: implications for a link between proteoglycans and diabetic disorders in the aortic valve. Diab. Vasc. Dis. Res. 2018: 1479164118817922. 2018/12/20. DOI: https://doi.org/10.1177/1479164118817922.
[69] Liu AC, Joag VR and Gotlieb AI. The emerging role of valve interstitial cell phenotypes in regulating heart valve pathobiology. *Am J Pathol* 2007; 171: 1407–1418. 2007/09/08. DOI: ajpath.2007.070251 [pii] 10.2353/ajpath.2007.070251.
[70] Otto CM, Kuusisto J, Reichenbach DD, et al. Characterization of the early lesion of 'degenerative' valvular aortic stenosis. Histological and immunohistochemical studies. *Circulation* 1994; 90: 844–853. 1994/08/01.
[71] B. Law, V. Fowlkes, J.G. Goldsmith, et al., Diabetes-induced alterations in the extracellular matrix and their impact on myocardial function, Microsc. Microanal. 18 (2012) 22–34, https://doi.org/10.1017/S1431927611012256.
[72] A. Aneja, W.H. Tang, S. Bansilal, et al., Diabetic cardiomyopathy: insights into pathogenesis, diagnostic challenges, and therapeutic options, Am. J. Med. 121 (2008) 748–757, https://doi.org/10.1016/j.amjmed.2008.03.046.
[73] van Heerebeek L, Hamdani N, Handoko ML, et al. Diastolic stiffness of the failing diabetic heart: importance of fibrosis, advanced glycation end products, and myocyte resting tension. *Circulation* 2008; 117: 43–51. 2007/12/12. DOI: https://doi.org/10.1161/CIRCULATIONAHA.107.728550.
[74] Fiaschi T, Magherini F, Gamberi T, et al. Hyperglycemia and angiotensin II cooperate to enhance collagen I deposition by cardiac fibroblasts through a ROS-STAT3-dependent mechanism. Biochim. Biophys. Acta 2014; 1843: 2603-2610. 2014/07/30. DOI: https://doi.org/10.1016/j.bbamcr.2014.07.009.
[75] V.P. Singh, K.M. Baker, R. Kumar, Activation of the intracellular renin-angiotensin system in cardiac fibroblasts by high glucose: role in extracellular matrix production, Am. J. Physiol. Heart Circ. Physiol. 294 (2008) H1675–H1684, https://doi.org/10.1152/ajpheart.91493.2007.
[76] Tokudome T, Horio T, Yoshihara F, et al. Direct effects of high glucose and insulin on protein synthesis in cultured cardiac myocytes and DNA and collagen synthesis in cardiac fibroblasts. *Metabolism* 2004; 53: 710–715. 2004/05/28.
[77] Zhang Y, Wang JH, Zhang YY, et al. Deletion of interleukin-6 alleviated interstitial fibrosis in streptozotocin-induced diabetic cardiomyopathy of mice through affecting TGFbeta1 and miR-29 pathways. Sci. Rep. 2016; 6: 23010. 2016/03/15. DOI: https://doi.org/10.1038/srep23010.